# New insights into the thermal reduction of graphene oxide: Impact of oxygen clustering

Priyank V. Kumar [a], [1], Neelkanth M. Bardhan [a], [b], [1], Guan-Yu Chen [c], [f], Zeyang Li [d], Angela M. Belcher [a], [b], [e], [**], Jeffrey C. Grossman [a], [*]

[a] Department of Materials Science and Engineering, Massachusetts Institute of Technology, Cambridge, MA 02139, USA
[b] The David H. Koch Institute for Integrative Cancer Research at the Massachusetts Institute of Technology, Cambridge, MA 02139, USA
[c] Institute of Biomedical Engineering, National Chiao Tung University, Hsinchu 300, Taiwan
[d] Whitehead Institute for Biomedical Research, Cambridge, MA 02142, USA
[e] Department of Biological Engineering, Massachusetts Institute of Technology, Cambridge, MA 02139, USA
[f] Department of Biological Science and Technology, National Chiao Tung University, Hsinchu 300, Taiwan

## ARTICLE INFO

## ABSTRACT

Graphene has attracted interest for a number of applications ranging from electronics, optoelectronics to membrane-based technologies. The thermal reduction of chemically exfoliated graphene oxide (GO) sheets represents an important step for large-scale, solution-based graphene synthesis. Therefore, understanding the reduction process and being able to provide new handles to control the resulting sheet properties is highly desirable. Using atomistic calculations combined with experiments, we study and demonstrate the impact of one such new handle — oxygen clustering on the graphene basal plane — on the structural and electrical properties of reduced GO (rGO) structures. Our calculations reveal that the number of oxygen and carbon atoms removed from the graphene plane during reduction can be tuned depending on the degree of oxygen clustering, without altering the reduction temperature. Further, we demonstrate that rGO thin films with improved sheet resistance (up to 2-fold smaller) can be obtained by facilitating oxygen clustering prior to reduction. Overall, our results highlight that oxygen clustering serves as a useful handle in controlling the structural and electrical properties of the resulting rGO structures, and could be potentially useful toward the synthesis of electrodes, graphene quantum dots and for different graphene-based thin film applications.

## 1. Introduction

Graphene is an atom-thick sheet of carbon possessing remarkable electronic properties and is emerging as a leading candidate for next-generation electronic devices [1]. The ability to produce graphene on a large scale and to control its deposition on a variety of substrates is crucial in this regard [2]. The chemical exfoliation of graphite to form solution-processable graphene oxide (GO) sheets, and their subsequent thermal reduction to reduced GO (rGO) through the restoration of graphitic characteristics is a promising step in this direction [3–5]. While rGO thin films have traditionally served as large-area, ultra-thin conductors in electronic devices, they are becoming increasingly popular for other applications including optoelectronics [3], catalysis [6], sensors [7] and filtration [8,9], where the tunable carbon–oxygen network and the ability to form porous ultra-thin layered membranes are highly desirable. As a result, developing ways to control the reduction of GO sheets with an aim to tailor the resulting sheet structure, chemistry and properties is of great importance.

Current thermal reduction protocols, however, depend largely on the reduction temperature as a suitable handle to control the sheet characteristics, i.e. they rely on *direct* reduction of as-synthesized GO sheets at different temperatures with no additional ways to control the process [10,11]. Given the importance of rGO in a number of applications, it is desirable to develop other useful handles, in addition to temperature, for tailoring the sheet structure and chemistry (carbon/oxygen concentration, relative functional group distribution etc.). It would be further beneficial if

such control knobs help us realize better sheet properties (such as lower sheet resistance, higher chemical reactivity etc.) compared to the ones being currently achieved through high temperature reduction alone.

Here, using a combination of atomistic computations supported by experiments, we demonstrate the advantages of one such handle, which involves facilitation of oxygen clustering in GO structures, prior to its reduction. Using atomistic simulations on realistic, disordered GO structures, we show that − at a constant reduction temperature − our strategy enables additional control over the residual carbon−oxygen content, along with tailoring the size and distribution of carbon vacancies (pores) created during the thermal reduction process. Further, by employing this strategy in our experiments, we are able to reduce the sheet resistance of rGO thin films by 30−50%, thereby representing a promising step toward the production of higher electrical quality graphene. Finally, we discuss the associated structural models and suggest suitable approaches to exercise effective control over the process of oxygen clustering in GO. Taken together, our results shed new insights on the reduction process of GO and provide suitable guidelines for designing GO/rGO structures for various applications.

## 2. Methods

### 2.1. Computational details

All Molecular Dynamics (MD) simulations were carried out using the LAMMPS package with the ReaxFF reactive force field [12,13]. For the thermal reduction simulations, we followed a procedure from previous computational works [2,14], where the temperature of the system containing GO structures was increased from 10 K to 1500 K over a time interval of 250 fs. The GO sheets were annealed at 1500 K for 250 ps to obtain rGO structures. The resulting by-products were removed from the simulation cell, and the rGO structure was further annealed at 300 K for 1.25 ps to confirm its stability.

To understand how oxygen clustering affects the nature of the carbon−oxygen bonds in GO structures, we performed additional simulations at 300 K. This was done using the same set of initial GO structures by following a similar procedure mentioned above, except that the temperature of the system was increased from 10 K to 300 K over a time interval of 250 fs, followed by annealing the GO structures at 300 K for 250 ps [15]. In all our simulations, we used a time step of 0.25 fs and the NVT Berendsen thermostat [2].

All the Density Functional Theory (DFT) calculations are performed with a plane-wave basis set as implemented in the VASP package [16,17]. We used the projector augmented wave method to describe the core electrons [18] and the Perdew-Burke-Ernzerhof exchange-correlation functional [19]. To understand unit processes controlling thermal reduction of GO, oxygen clusters (1−4 oxygen atoms) were modeled on a periodic graphene sheet with 128 carbon atoms, large enough to prevent any interaction with their images. To study the impact of N-doping on the oxygen clustering process, we used N-doped GO structures constructed using a 4 × 0.8 nm graphene sheet consisting of 64 C atoms. The structures were relaxed to less than 0.03 eV A$^{-1}$, and a wave-function kinetic energy cutoff of 500 eV was used, with a gamma-point *k*-grid. A vacuum region of 16 Å was used in the direction normal to the graphene sheets.

### 2.2. Experimental details

GO solutions (4 mg/ml, in water) were purchased from Sigma Aldrich (product #777676). Two types of thin films were prepared: 1) GO films produced through drop-casting onto silicon substrates,

and 2) Free-standing GO thin films produced through the vacuum filtration technique. In case of the former, 100 μL of the stock solution (4 mg/ml) was deposited on silicon substrates forming ~2 μm-thick films (~1 cm in diameter). In case of the latter, 2 ml of the stock solution (4 mg/ml) was further diluted by adding 8 ml of distilled water. The resulting solution was vacuum-filtered to obtain ~10 μm-thick films (~2.5 cm in diameter). Both these thin films were dried overnight at room temperature. The freestanding circular GO film of ~2.5 cm in diameter was cut down into four equal parts, and each of these parts was used as a sample. The films were subjected to mild annealing at 80°C in a temperature-controlled oven (air atmosphere) for a course of nine days to facilitate oxygen clustering (or $sp^2$ clustering), a procedure employed by us previously [15]. Samples were retrieved at intervals of one, five and nine days, to obtain GO thin film samples with varying degree of $sp^2$ clustering with the day 0 sample showing no clustering, while the day 9 sample showing the greatest degree of clustering as demonstrated in our previous work [15]. The retrieved thin film samples were subjected to thermal reduction at elevated temperatures in a temperature-controlled oven (air atmosphere) for 20 min. We evaluated the electrical properties of rGO thin films using four-point probe transport measurements, conducted at room temperature.

## 3. Results and discussion

### 3.1. Structural evolution during the reduction of GO with varying degree of oxygen clustering: thermal annealing at 1500 K

We carried out a combination of classical molecular dynamics (MD) simulations and density functional theory (DFT) calculations to understand the impact of oxygen clustering on the structural and chemical evolution of GO thin films during thermal reduction. For our MD simulations, model GO structures with different sizes of oxidized and graphitic domains (none, three and six graphene rows) were prepared with the oxygen concentration kept fixed to mimic the oxygen clustering process (Fig. 1a), based on a model developed by us previously [15]. The row 0, row 3 and row 6 cases were constructed to compare GO models with no oxygen clustering, partial oxygen clustering and extensive oxygen clustering, respectively (see Fig. 1a for more details). Briefly, the oxidized domains consisted of randomly distributed epoxy and hydroxyl groups attached to both sides of the graphene sheet [20]. Different oxygen concentrations (10 and 20 at%) and fraction of epoxy to hydroxyl groups (3:2 and 2:3) were tested to study the effect of such local variations on the reduction behavior of GO films [2,14,15]. A 3 × 1.3 nm periodic graphene sheet was used for all simulations. We used ten samples for each composition, which allows us to present meaningful averages of the computed properties.

Thermal reduction simulations were carried out at 1500 K (see Methods). The number of oxygen and carbon atoms removed from the GO structure during the MD thermal reduction runs is shown in Fig. 1b as a function of different graphitic domain sizes (in other words, as a function of increasing oxygen clustering). Since GO has different local oxygen concentrations and functional group distribution, it is important to understand the impact of clustering in connection to these two factors. At high oxygen contents, our results show that not only does the number of oxygen atoms removed increases, but also the number of carbon atoms removed from the graphene backbone increases with increasing degree of oxygen (or $sp^2$) clustering. At lower oxygen contents, i.e. 10 at%, we observed that the $sp^2$ clustering has weaker effects on increasing the carbon and oxygen removal, although the effects still persist.

Our simulations also capture the effects of having different oxygen functional groups in the oxidized domain. They show that the
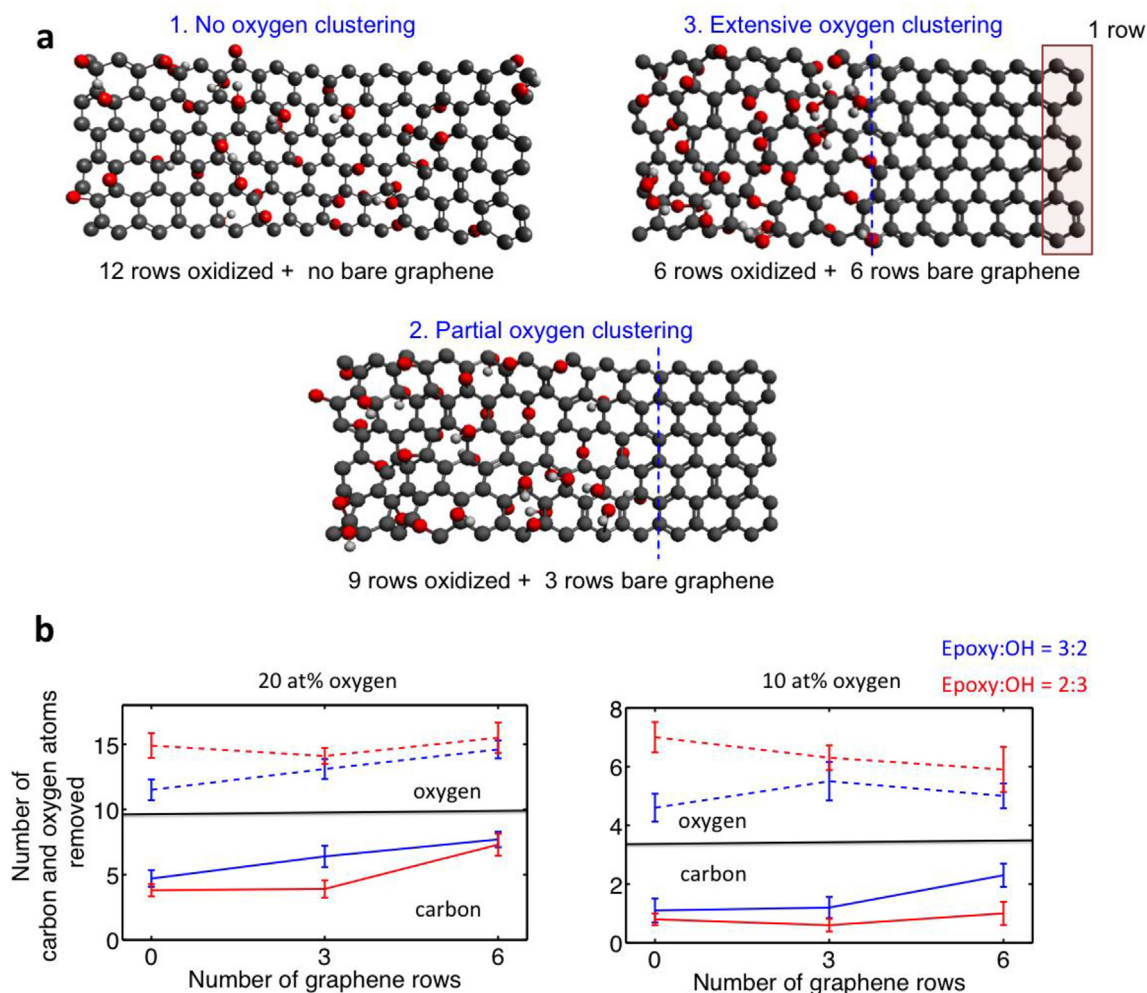
**Fig. 1. Carbon and oxygen removal during the reduction of GO structures with increasing degree of oxygen clustering.** a) Representative model GO structures used to study the effect of oxygen clustering on the thermal reduction behavior of GO structures in MD simulations. Each structure consists of two distinct oxidized and graphene phases with different domain sizes, mimicking different degrees of oxygen clustering. The first structure has no graphene rows indicating no oxygen clustering, while the second and the third structures represent partial and extensive oxygen clustering, respectively. Carbon, oxygen and hydrogen are represented as gray, red and white spheres, respectively. b) The number of oxygen and carbon atoms removed during thermal reduction, both showing an increasing trend with increasing number of graphene rows (or increasing degree of oxygen clustering). The effect is pronounced for GO structures with high local oxygen concentrations and epoxy-rich domains. (A color version of this figure can be viewed online.)

epoxy-rich GO domains are more influenced by oxygen clustering, in that they tend to lose more carbon and oxygen atoms with increasing oxygen clustering, even for cases with lower oxygen concentrations. This result highlights the importance of functional group distribution in GO and provides additional guidelines for controlling the structural properties of resulting rGO structures.

It should be noted that such structural variations have been previously attained when the reduction temperature is used as a control knob [2,10]. In our case here, we observe that changes in the carbon and oxygen concentration can be achieved – at the same reduction temperature – by simply facilitating oxygen clustering on the graphene basal plane prior to reduction. These results thus demonstrate that controlling the degree of oxygen clustering in GO structures can be an effective way to tune the local residual oxygen and carbon content in the corresponding rGO structures.

Our simulations also point toward other interesting results. We found that the formation of pores (a cluster of carbon vacancies) decorated with oxygen atoms at the periphery, becomes increasingly favorable with oxygen clustering, which follows from our previous discussion on increasing carbon removal with oxygen clustering. This result is important since it demonstrates that

oxygen clustering could serve as a useful control parameter for the design of next-generation graphene-based porous membranes, which have garnered tremendous attention recently [8,9,21,22]. Thus far, such membranes have been fabricated by *directly* reducing as-synthesized GO thin films [8,9], while use of procedures to facilitate oxygen clustering prior to reduction can lead to interesting membrane properties, that currently remain unexplored.

### 3.2. Impact of oxygen clustering on carbon–oxygen bonding in GO: thermal annealing at 300 K

In light of the insights obtained from the high temperature reduction simulations, it is critical to understand if and how oxygen clustering influences the carbon–oxygen bonding environment in GO structures even before it is subjected to reduction. It is important to ascertain if the driving force for oxygen and carbon removal is derived from the mere difference in the arrangement of oxygen atoms on the graphene plane.

In this regard, we carried out additional MD simulations to specifically understand how oxygen clustering affects the carbon––oxygen bond length distribution (and correspondingly their bond

strength) in GO structures at room temperature. These simulations were performed on the same set of structural models considered before, but annealing was performed at 300 K to simulate room temperature behavior (see Methods). After equilibration, we obtained the C—O bond length distribution from the corresponding GO structures. Fig. 2 shows an example C—O bond length distribution plot comparing the two cases: 1) when oxygens are present in randomly distributed (row O case), and 2) when the oxygens are present in a highly clustered state (row 6 case). In this example, the oxygen concentration is 20 at% and the epoxy to hydroxyl group ratio is 3:2. Interestingly, oxygen clustering has a significant effect on the nature of C—O bonds in GO structures, evident from the changes in the C—O bond distribution at a constant oxygen concentration. Our analysis shows that when oxygen atoms are present in a clustered form, a larger fraction of the C—O bonds are below 1.4 Å (42%), compared to 28% for the distributed case. This suggests that a larger fraction of the oxygen functional groups prefer to form carbonyl groups (C=O) when oxygen atoms are present in proximity, in favor of the epoxy groups (C—O—C) when they are present in a distributed form. Given the larger fraction of C=O bonds, this result shows that it is easier for carbon to be removed at higher temperatures in the form of CO molecules. Besides, it also shows that the chemistry of GO sheets can be altered by simply changing the degree of oxygen clustering in GO, without disturbing the overall oxygen content.

We further find that a larger fraction of the C—O bonds are above 1.6 Å (18%) for the clustered case compared to the distributed case (3%), revealing the presence of a greater number of weaker C—O bonds when the oxygen atoms are present in a clustered form. This demonstrates easier removal of such oxygen groups when subjected to reduction at elevated temperatures, consistent with higher oxygen removal in the clustered case in our reduction simulations (at 1500 K). Collectively, these results show how C—O bonds can be weakened and oxygen clustering by itself provides partial driving force for the removal of oxygen functional groups,

without needing impetus from the external temperature.

### 3.3. Understanding unit processes: DFT calculations

To further understand unit processes favoring oxygen removal in addition to the consumption of the carbon backbone, we carried out DFT calculations of the reaction pathways that lead to the reduction of GO. Specifically, we considered removal of (1) $O_2$ (2) CO and (3) $CO_2$ molecules from the initial GO structures; the last two being responsible for the consumption of the carbon backbone [23,24]. The initial GO configurations were constructed with one (1-O), two (2-O), three (3-O) and four (4-O) neighboring oxygen atoms to model different degrees of oxygen clustering. We considered two possibilities for each cluster model: 1) when oxygen atoms cluster on the same side, and 2) when oxygen atoms cluster on both sides. Fig. 3a shows an example set of cluster models used when oxygen atoms are on the same side. The generation of $O_2$, CO and $CO_2$ molecules from each of these configurations was studied leading to different product structures (see Supplementary Fig. S1 for the product structures).

We assessed the favorability of the reactions by computing the energy difference between the final and initial configurations, as shown in Fig. 3b. First, we note that oxygen removal in the form of an $O_2$ molecule is diffusion-limited in the case of isolated oxygen atoms (1-O case, no clustering), i.e. oxygen atoms have to diffuse around and find a neighboring oxygen atom to form an $O_2$ molecule. Instead, upon partial clustering (2-O case, when oxygen atoms are present on the same side), the formation of an $O_2$ molecule is no longer diffusion-limited, and removal of oxygen in the form of $O_2$ is favored thermodynamically by a reduction in the total energy of 1.44 eV. On the other hand, removal of oxygen through the other two reaction channels, i.e. in the form of CO and $CO_2$ molecules, remains thermodynamically unfavorable in the 1-O and 2-O cases.

Upon further clustering of oxygen (3-O and 4-O cases), competing reaction channels that generate CO and $CO_2$ molecules
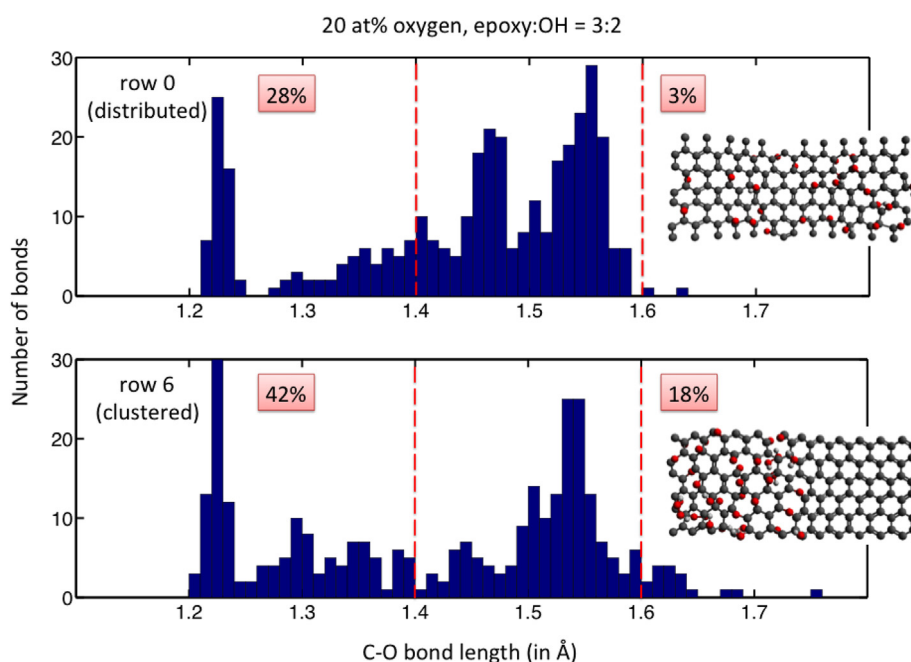


**Fig. 2. Impact of oxygen clustering on the carbon—oxygen bonding environment in GO structures.** Plots showing changes in the C—O bond length for two cases: oxygens are randomly distributed (row 0) and oxygens are highly clustered (row 6). For the example chosen, oxygen concentration is 20 at% and the epoxy to hydroxyl ratio is 3:2. The fraction of C—O bonds present below 1.4 Å and above 1.6 Å is also shown. These numbers reveal that 1) a greater fraction of C—O bonds are present as carbonyls and 2) a greater fraction of the C—O bonds are weakened, when oxygen atoms form clusters rather than being randomly distributed. (A color version of this figure can be viewed online.)
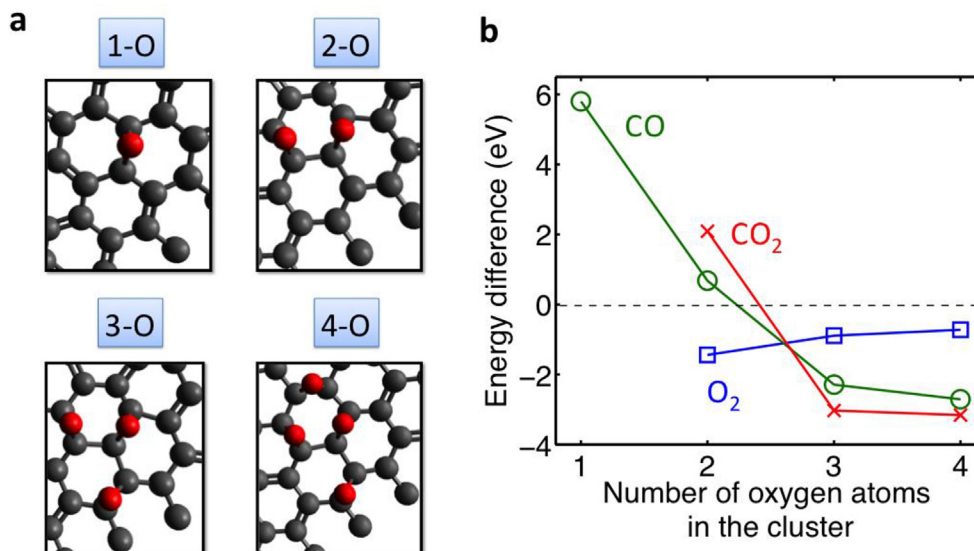
**Fig. 3. Assessing the favorability of unit reduction reactions with increasing degree of oxygen clustering using DFT calculations**. a) Initial configurations with one, two, three and four neighboring oxygen atoms used to model reduction reactions (oxygen atoms clustering on the same side). b) The energy differences (in eV) between the final and the initial configurations ($E_f − E_i$) listed for three reactions − removal of $O_2$, CO and $CO_2$ from the initial configurations shown in (a). These results show that with increasing clustering of oxygen, removal of both oxygen and carbon in the form of CO and $CO_2$ becomes increasingly favorable, thereby leading to the consumption of carbon backbone and leaving behind vacancies (and holes). (A color version of this figure can be viewed online.)

are favored more than $O_2$ evolution. Similar results were obtained for the case when oxygen atoms were present on both the sides (see Supplementary Fig. S2). In addition to favorable thermodynamics, previous DFT calculations have reported favorable kinetics for such reactions as well [23]. The activation barrier for CO and $CO_2$ removal is known to decrease by a factor of up to three when oxygens are present in proximity (from ~1.8 eV to ~0.6 eV) [23]. These reactions consume the carbon backbone, and leave behind defects (single vacancies and holes) in rGO films. The surrounding oxygen atoms help saturate the carbon dangling bonds created due to a carbon vacancy, which explains why these reactions become favorable with increasing degree of oxygen clustering [23].

### 3.4. Electrical properties of rGO thin films

It should be recalled that oxygen clustering in GO could also be viewed as clustering and formation of distinct $sp^2$ domains. While we concentrated mainly on the oxidized domains in the previous sections, we explore the benefits of $sp^2$ clustering on the reduction of GO structures here. From our structural models, we envisioned that the rGO films produced from GO structures containing larger and well-connected $sp^2$ domains could lead to better electrical properties, compared to rGO films obtained through direct reduction of GO. This is important because a well known limitation of the direct thermal reduction protocol is that it leads to a spatial distribution of $sp^3$ sites in the graphene lattice that restricts the expansion of the $sp^2$ phase, resulting in inferior electrical properties of rGO compared to mechanically exfoliated graphene [25,10].

In order to test our hypothesis of obtaining better electrical characteristics, we carried out experiments wherein oxygen clustering was initiated in as-synthesized GO samples by mildly annealing the GO films at 80 °C for up to 9 days, a process employed by us previously [15]. This results in the expansion and formation of distinct $sp^2$ domains on the order of 1−2 nm [15]. The GO films were then subjected to thermal reduction at elevated temperatures (see Methods). A schematic of the experimental procedure used in our study is shown in Fig. 4a.

Fig. 4b compares the sheet resistance values of control rGO films (day 0) with those of the *modified*-rGO films (day 1−9), for a reduction temperature of 350°C. In agreement with our hypothesis, we did observe a sharp drop in the sheet resistance values with pretreatment time at these reduction temperatures. Electrical measurements reveal 30−50% reduction in the sheet resistance values of the *modified*-rGO films (drop cast onto silicon substrates), compared to the control rGO sample. Similarly, we performed experiments on free-standing GO thin films (see Supplementary Fig. S3), where we observed a drop in the sheet resistance values by 20−40%. These results show that the mild annealing procedure employed here is useful to derive crucial insights regarding the impact of oxygen clustering on the electrical properties of rGO thin films.

### 3.5. Schematic model

Based on our study, we present a structural model of GO subjected to the process of oxygen clustering, followed by thermal reduction. In as-synthesized GO structures, the oxygen atoms are randomly distributed across the graphene plane, and when subjected to a suitable external stimulus (such as mild temperatures), they start to diffuse and form clusters, gradually leading to two distinct phases, graphitic and oxidized domains. This process is represented schematically in Fig. 5 (top panel), depicting different degree of oxygen clustering over the nine days of mild annealing.

In Fig. 5 (bottom panel), structural evolution during the reduction of as-synthesized and *modified*-GO structures is depicted: (control-rGO) The structure of rGO obtained directly from as-synthesized GO shows oxygen atoms and carbon vacancies distributed randomly across the graphene plane, thereby leading to discontinuous $sp^2$ phases and poorer electrical conductivity (*modified*-rGO). The reduction of GO structures with increasing oxygen clustering shows larger $sp^2$ clusters facilitating greater connectivity, which correlates to lower sheet resistance in our experiments. At high enough reduction temperatures, these rGO structures also depict a higher degree of carbon and oxygen removal with progressively increasing oxygen clustering, as evidenced in our atomistic simulations, which could lead to creation of
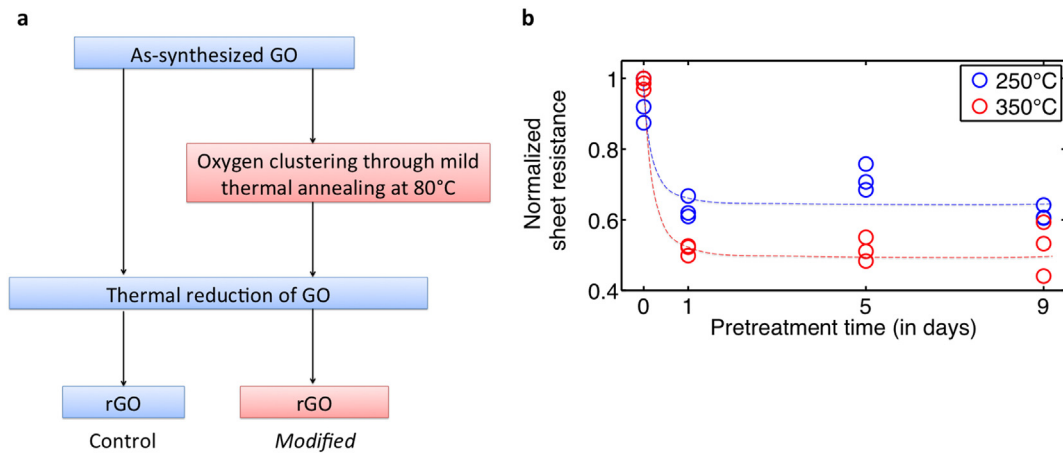
**a**



**b**



**Fig. 4. Electrical measurements on rGO thin films.** a) Schematic of the experimental procedure employed. b) Sheet resistances of *modified*-rGO thin films (day 1–9) prepared by drop-casting show reduced values compared to that of the control rGO sample (day 0). The trend is represented by the dotted lines and the reduction temperatures are listed. (A color version of this figure can be viewed online.)
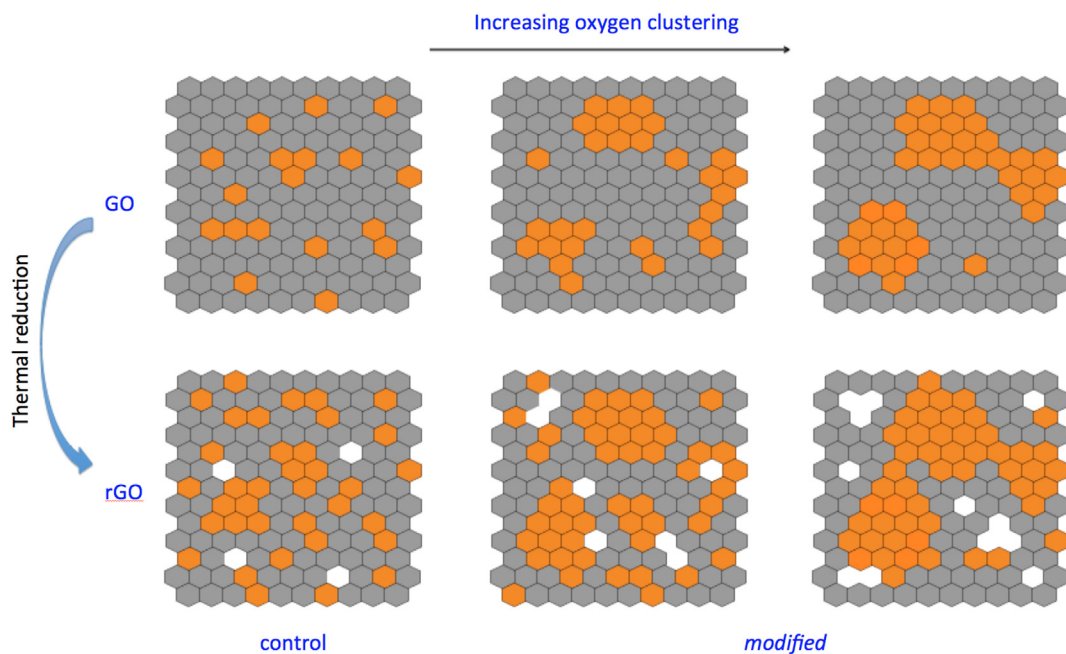


**Fig. 5. Structural models of rGO obtained from GO films at different stages of the oxygen clustering process.** The upper panel shows the formation of distinct oxidized and graphitic domains (different degrees of oxygen clustering) in GO structures. The graphitic domains are represented by orange, while the oxidized domain is represented by gray. The bottom panel shows the corresponding rGO structures obtained after thermal reduction. The *modified*-rGO structures show larger $sp^2$ clusters compared to the control sample. Also, importantly, at high enough reduction temperatures, they show an increasing degree of oxygen and carbon removal leading to a higher concentration of carbon vacancies and holes compared to the control rGO structure (obtained through the direct reduction of as-synthesized GO structures). (A color version of this figure can be viewed online.)

larger pores and processes such as oxidative cutting of graphene sheets.

In connection to the structural model presented above, it is interesting to note that the electrical properties of corresponding rGO structures obtained by high temperature thermal annealing rather saturate after day 1 − day 5. We attribute this to the nature of electrical conductivity in rGO films. The electrical conductivity in GO is well known to be governed by a hopping model, thereby exhibiting an exponential dependence on the $sp^2$ cluster size [10]. Therefore, the electrical conductivity in GO increases by up to 4 orders of magnitude from day 0 to day 9 upon mild thermal annealing (see Ref. [15]). On the other hand, the electrical conductivity in rGO is known to be governed by a percolation model

and thus exhibits a power law dependence on the $sp^2$ fraction [10]. This means that although we may increase the $sp^2$ cluster size in rGO by the same amount as with the case of GO, we would measure a much smaller change in the conductivity of rGO films as evidenced in this work, going from day 0 (control) to the *modified*-rGO samples. Further, different factors at play such as the presence of amorphous hydrocarbons on the surface could cause variations in the sheet resistance data [2,26]. In spite of such factors, we still find reduction in sheet resistance values, highlighting the importance of creating larger $sp^2$ clusters in enhancing the electrical quality of rGO films [10].

### 3.6. Strategies to control oxygen clustering

We have demonstrated that mild thermal annealing, carried out at 50—80 °C for 1—9 days can induce oxygen clustering through diffusion of oxygen functional groups on the basal plane [15]. While this is a useful procedure, the high diffusion barrier for epoxide groups (0.83 eV, Fig. 6a) and the lack of spatial control on the oxidized domains can be limitations. To this end, it would be desirable to (1) expedite the process of oxygen clustering by lowering the activation barrier for epoxy diffusion, and (2) exercise control over the positioning of oxygen domains on the basal plane. In what follows, we show that it is possible to obtain such control by carefully doping GO sheets with nitrogen atoms. Our calculations show that N-doping of GO sheets can significantly lower the activation barrier associated with the diffusion of epoxy groups

(Fig. 6b). Depending on the positioning of the N atom relative to the diffusing epoxy group, certain cases could even lead to a barrierless diffusion of epoxy groups, suggesting that N-doping is an effective route towards controlling the kinetics of oxygen clustering in GO.

In order to investigate the possibility of exercising spatial control over the oxygen atoms, additional DFT calculations were performed by considering oxidized domains of different compo-sitions ($C_2O$, $C(OH)$ and $C_4O(OH)_2$) in the vicinity of N-dopants (see Methods). We computed the energetics of these structures by systematically varying the separation between N-dopants and the oxidized regions (Fig. 6c). We also varied the dopant concentration (1 and 2 N atoms) in our calculations. In all cases, we find that the structures with least separation between the N-dopants and oxidized domains are energetically favored. This indicates favorable clustering of oxygen atoms closer to the N-dopants as opposed to
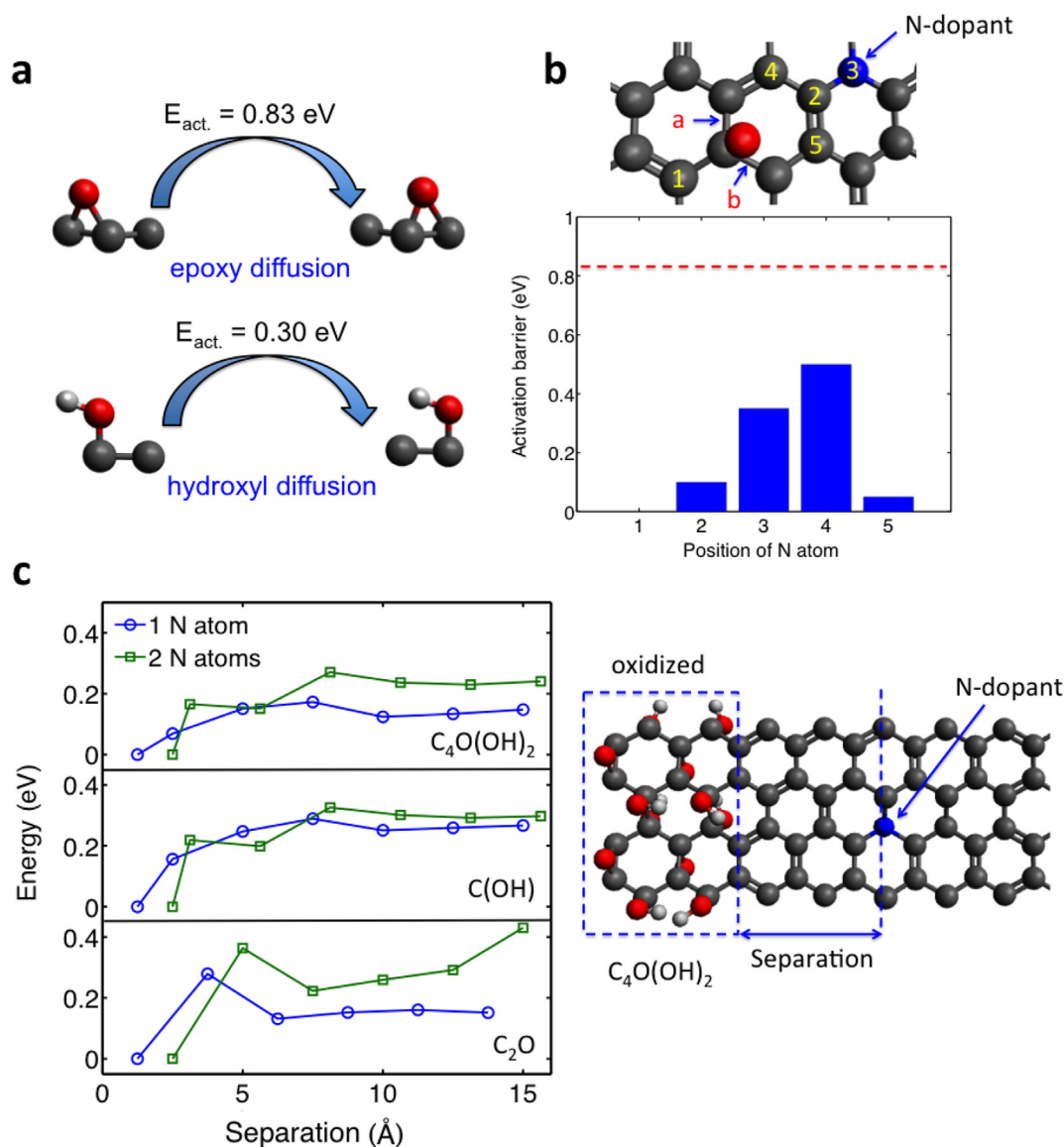


**Fig. 6. Effective control of the oxygen clustering process.** (a) Computed activation barriers for the diffusion of epoxy and hydroxyl functional groups on the graphene basal plane. (b) Controlling the diffusion of epoxy functional group *via* N-doping. The plot shows computed activation barriers for the diffusion of a single epoxy group from bridge site-a to bridge site-b, for different positions of the N-dopant (blue sphere). As shown, the computed barriers are well below the pure graphene case of 0.83 eV (dashed red line). (c) Controlling the positioning of phase separated oxidized domains *via* N-doping. The plot reveals that it is energetically more favorable for oxygen atoms to cluster close to N-dopants than to cluster farther away from them. For each cluster composition, calculations using two N concentrations (1 and 2 N atoms) are reported and the energy values are referenced to the most stable structure, which turns out to be the case when the N-dopant is closest to the oxidized domain in all of the studied structures. A representative N-doped GO structure is shown alongside for reference. (A color version of this figure can be viewed online.)

farther away from them, meaning that it should be possible to exercise spatial control over the oxidized domains by manipulating the positioning of N-dopants along the basal plane.

An additional way to control oxygen diffusion was reported by Suarez et al. [27]. They showed that the diffusion barrier for the epoxy group decreases to values as low as 0.15 eV upon application of a suitable gate voltage. Overall, the application of such external stimuli is promising; in that they not only accelerate oxygen diffusion, but also provide considerable opportunities to control the positioning of the oxidized domains in GO. Further high-temperature reduction of such tailored GO sheets could offer routes to tune the optical and electronic properties of rGO sheets in unique ways.

It should be noted that while our combined DFT and MD studies help interpret structural evolution at the atomic scale, they do have certain limitations. The reduction temperature of 1500 K used in our simulations to expedite the kinetics is well above the temperatures commonly employed in experiments, and we further neglect the presence of surface residue in our simulations, which could impact the properties of rGO films in additional ways. A high degree of oxygen clustering has been shown to lead to complex reconstructions in GO structures [23]. Hence, modeling realistic GO structures with a high degree of oxygen clustering is challenging and may involve additional processes such as oxidative cutting forming graphene quantum dots [28], charring [29] and generation of by-products other than CO and $CO_2$ as observed in the case of amorphous carbon systems [30]. Recent *ab initio* and MD simulations based on ReaxFF potentials have predicted the evolution of small-molecule hydrocarbons ($C_mH_n$) and other molecular fragments containing oxygen ($C_mH_nO$) alongside CO and $CO_2$, when carbon-based phenolic resins are heated [29–32]. While such finer details are not captured in our simulations owing to simpler initial configurations, they nevertheless provide important topics for future exploration. Another interesting direction to explore would be to understand the impact of oxygen clustering on chemical reduction of GO thin films. The mechanisms associated with chemical reduction are distinct from the ones observed here with thermal reduction [11,33,34], and could lead to other interesting insights. Yet, utilizing the subset of rGO structures considered here, we are able to gain important understanding related to the effects of oxygen clustering on carbon and oxygen removal from GO.

## 4. Conclusion

In summary, our theoretical analyses show that oxygen clustering in GO serves as a suitable handle toward controlling the structure, chemistry and sheet properties of the resulting rGO sheets. Specifically, we demonstrate enhanced oxygen and carbon removal upon oxygen clustering, which can be used to control the residual oxygen content and pore formation in rGO, without having to alter the reduction temperature. Our electrical measurements suggest that rGO sheets with superior electrical characteristics can be fabricated by facilitating oxygen clustering in GO prior to its reduction, highlighting the importance of increasing the $sp^2$ domain size. Finally, we show controlled N-doping as a suitable way to expedite oxygen clustering and manipulate the positioning of the oxidized domains. These results are critical, in that they represent a first step in highlighting the advantages of using additional handles other than employing reduction temperature alone to reduce as-synthesized GO films. Our strategy could open up novel routes toward the production of rGO structures at lower temperatures, synthesis of graphene quantum dots and development of graphene for membrane applications.

## Appendix A. Supplementary data

Supplementary data related to this article can be found at http://dx.doi.org/10.1016/j.carbon.2015.12.087.

## References

[1] A.K. Geim, K.S. Novoselov, The rise of graphene, Nat. Mater. 6 (2007) 183–191.
[2] A. Bagri, et al., Structural evolution during the reduction of chemically derived graphene oxide, Nat. Chem. 2 (2010) 581–587.
[3] G. Eda, M. Chhowalla, Chemically derived graphene oxide: towards large-area thin-film electronics and optoelectronics, Adv. Mater. 22 (2010) 2392–2415.
[4] G. Eda, G. Fanchini, M. Chhowalla, Large-area ultrathin films of reduced graphene oxide as a transparent and flexible electronic material, Nat. Nanotechnol. 3 (2008) 270–274.
[5] W.S. Hummers, R.E. Offeman, Preparation of graphitic oxide, J. Am. Chem. Soc. 80 (1958), 1339–1339.
[6] J. Pyun, Graphene oxide as catalyst: application of carbon materials beyond nanotechnology, Angew. Chem. Int. Ed. 50 (2011) 46–48.
[7] K.P. Loh, Q. Bao, G. Eda, M. Chhowalla, Graphene oxide as a chemically tunable platform for optical applications, Nat. Chem. 2 (2010) 1015–1024.
[8] H.W. Kim, et al., Selective gas transport through few-layered graphene and graphene oxide membranes, Science 342 (2013) 91–95.
[9] H. Li, et al., Ultrathin, molecular-sieving graphene oxide membranes for selective hydrogen separation, Science 342 (2013) 95–98.
[10] C. Mattevi, et al., Evolution of electrical, chemical, and structural properties of transparent and conducting chemically derived graphene thin films, Adv. Funct. Mater. 19 (2009) 2577–2583.
[11] S. Pei, H.-M. Cheng, The reduction of graphene oxide, Carbon 50 (2012) 3210–3228.
[12] S. Plimpton, Fast parallel algorithms for short-range molecular dynamics, J. Comput. Phys. 117 (1995) 1–19.
[13] A.C.T. van Duin, S. Dasgupta, F. Lorant, W.A. Goddard, ReaxFF: a reactive force field for hydrocarbons, J. Phys. Chem. A 105 (2001) 9396–9409.
[14] P.V. Kumar, M. Bernardi, J.C. Grossman, The impact of functionalization on the stability, work function, and photoluminescence of reduced graphene oxide, ACS Nano 7 (2013) 1638–1645.
[15] P.V. Kumar, et al., Scalable enhancement of graphene oxide properties by thermally driven phase transformation, Nat. Chem. 6 (2014) 151–158.
[16] G. Kresse, J. Furthmüller, Efficient iterative schemes for ab initio total-energy calculations using a plane-wave basis set, Phys. Rev. B 54 (1996) 11169–11186.
[17] G. Kresse, J. Furthmüller, Efficiency of ab-initio total energy calculations for metals and semiconductors using a plane-wave basis set, Comput. Mater. Sci. 6 (1996) 15–50.
[18] G. Kresse, D. Joubert, From ultrasoft pseudopotentials to the projector augmented-wave method, Phys. Rev. B 59 (1999) 1758–1775.
[19] J.P. Perdew, K. Burke, M. Ernzerhof, Generalized gradient approximation made simple, Phys. Rev. Lett. 77 (1996) 3865–3868.
[20] J.T. Paci, T. Belytschko, G.C. Schatz, Computational studies of the structure, behavior upon heating, and mechanical properties of graphite oxide, J. Phys. Chem. C 111 (2007) 18099–18111.
[21] R.K. Joshi, et al., Precise and ultrafast molecular sieving through graphene oxide membranes, Science 343 (2014) 752–754.
[22] D. Cohen-Tanugi, J.C. Grossman, Water desalination across nanoporous graphene, Nano Lett. 12 (2012) 3602–3608.
[23] T. Sun, S. Fabris, S. Baroni, Surface precursors and reaction mechanisms for the thermal reduction of graphene basal surfaces oxidized by atomic oxygen, J. Phys. Chem. C 115 (2011) 4730–4737.
[24] R. Larciprete, et al., Dual path mechanism in the thermal reduction of graphene oxide, J. Am. Chem. Soc. 133 (2011) 17315–17321.
[25] C. Gómez-Navarro, et al., Electronic transport properties of individual chemically reduced graphene oxide sheets, Nano Lett. 7 (2007) 3499–3503.
[26] G. Eda, et al., Graphene oxide gate dielectric for graphene-based monolithic

field effect transistors, Appl. Phys. Lett. 102 (2013) 133108.

[27] A.M. Suarez, L.R. Radovic, E. Bar-Ziv, J.O. Sofo, Gate-voltage control of oxygen diffusion on graphene, Phys. Rev. Lett. 106 (2011) 146802.

[28] T. Sun, S. Fabris, Mechanisms for oxidative unzipping and cutting of graphene, Nano Lett. 12 (2012) 17–21.

[29] D. Jiang, A.C.T. van Duin, W.A. Goddard, S. Dai, Simulating the initial stage of phenolic resin carbonization via the ReaxFF reactive force field, J. Phys. Chem. A 113 (2009) 6891–6894.

[30] T. Qi, C.W. Bauschlicher, J.W. Lawson, T.G. Desai, E.J. Reed, Comparison of ReaxFF, DFTB, and DFT for phenolic pyrolysis. 1. Molecular dynamics simulations, J. Phys. Chem. A 117 (2013) 11115–11125.

[31] C.W. Bauschlicher, et al., Comparison of ReaxFF, DFTB, and DFT for phenolic pyrolysis. 2. Elementary reaction paths, J. Phys. Chem. A 117 (2013) 11126–11135.

[32] F.S. Movahed, G. Cheng, B.S. Venkatachari, & I. Cozmuta, in 42nd AIAA Thermophysics Conference (American Institute of Aeronautics and Astronautics). at <http://arc.aiaa.org/doi/abs/10.2514/6.2011-3786>.

[33] X. Gao, J. Jang, S. Nagase, Hydrazine and thermal reduction of graphene oxide: reaction mechanisms, product structures, and reaction design, J. Phys. Chem. C 114 (2010) 832–842.

[34] Y. Su, X. Gao, J. Zhao, Reaction mechanisms of graphene oxide chemical reduction by sulfur-containing compounds, Carbon 67 (2014) 146–155.